



NOTE

Internal Medicine

Computed tomography of thoracic lymph nodes in 100 dogs with no abnormalities in the dominated area

Hideki KAYANUMA^{1)*}, Kaoruko YAMADA¹⁾, Takuya MARUO¹⁾ and Eiichi KANA²⁾¹⁾Department of Veterinary Radiology, School of Veterinary Medicine, Azabu University, 1-17-71, Fuchinobe, Chuo, Sagami-hara, Kanagawa 252-5201, Japan²⁾Department of Small Animal Surgery, School of Veterinary Medicine, Azabu University, 1-17-71, Fuchinobe, Chuo, Sagami-hara, Kanagawa 252-5201, Japan

ABSTRACT. In dogs, reports on thoracic lymph nodes are lacking compared to abdominal lymph nodes. This report analyzed the position, number, size, shape, and homogeneity of thoracic lymph nodes (cranial sternal, cranial mediastinal, tracheobronchial, aortic thoracic, and pulmonary lymph nodes) using thoracic computed tomography (CT) images of 100 dogs without any lesions in the dominated areas of thoracic lymph nodes. The position and number of intrathoracic lymph nodes could be observed in CT, consistent with macroscopic anatomical studies. It was difficult to set a clinical index associated with size using CT scans. Image findings that indicated abnormalities, such as circular shapes and non-uniform, may be routinely found in dogs and may not be considered abnormal on CT scans.

KEY WORDS: canine, computed tomography, thoracic lymph node

J. Vet. Med. Sci.

82(3): 279–285, 2020

doi: 10.1292/jvms.19-0413

Received: 25 July 2019

Accepted: 26 December 2019

Advanced Epub:

23 January 2020

Lymph nodes are immune system organs found along the lymphatic vessels, and function as a wall against infections and tumor growth. Therefore, in cases of infection, neoplastic diseases, and inflammatory response in the branching network of lymphatic vessels, result in swollen lymph nodes. Since findings in the lymph nodes, such as enlargement, irregularity, hardness, and adhesion indicate neoplastic lesions, evaluation of regional lymph nodes is important in the staging of neoplastic diseases [5]. Therefore, diagnostic image findings, such as sizes, shapes, and homogeneity of lymph nodes determine the presence of infections, neoplastic diseases, and inflammatory responses. Case reports and studies are reported based on X-ray, ultrasound, and X-ray computed tomography (CT) imaging. However, X-ray examination cannot visualize normal lymph nodes in the thorax and the abdomen. Even when these lymph nodes are enlarged, they are difficult to discriminate from other structures. With ultrasound, lymph nodes near the skin and abdominal lymph nodes have been studied, and a number of findings may indicate malignancy [4, 9, 10–13]. These include enlargement of lymph nodes, increased number of lymph nodes, morphological change to a circular shape, decreased echogenicity, heterogeneity, irregular margins, and detection of vascular flow [4, 7, 9, 10–13]. However, as soundwaves are reflected by the gas in the thorax, ultrasound is usually ineffective for the examination of thoracic lymph nodes. Alternatively, resolution of CT scans and magnetic resonance imaging (MRI) is high, which makes them well suited for detection of small structures, such as lymph nodes. However, MRI is less practical since it is more time consuming and has a smaller imaging range compared to CT scans. On the other hand, CT can produce images in a relatively short period of time and cover a wider range, with little impact from respiratory movements. Thus, in evaluation of lymph nodes, CT is the most useful method. Though there are reports of the number, shape, and positions of normal abdominal lymph nodes in CT examination [2], there such studies on normal thoracic lymph nodes in dogs are limited [1]. Therefore, we analyzed thoracic CT images from 100 asymptomatic dogs and examined characteristics of thoracic lymph nodes.

We examined 100 dogs (52 males [12 unneutered and 40 neutered] and 48 females [10 unspayed and 38 spayed]) with mean age, 10.2 ± 2.38 years (range, 4–15 years; median, 10 years) and mean body weight of 14.5 ± 10.4 kg (range, 2.8–50 kg; median, 10.1 kg) at the Azabu University Veterinary Teaching Hospital, Kanagawa, Japan between February 2013 and August 2014. Their thoracic CT images and medical records confirmed no abnormalities or lesions in the dominated area of the thoracic lymph nodes. The breakdown of breeds was as follows: Miniature Dachshund (15), Labrador Retriever (10), Shih Tzu (7), Pembroke Welsh Corgi (5), Shetland Sheepdog (5), Chihuahua (5), Shiba Inu (4), Toy Poodle (4), Golden Retriever (3), Flat-Coated Retriever (3), Miniature Schnauzer (3), Jack Russell Terrier (2), Papillon (2), Miniature Pinscher (2), Irish Setter (1), Akita (1), German Shepard (1), Dalmatian (1), Bernese Mountain Dog (1), Pug (1), Basenji (1), Bearded Collie (1), Beagle (1), Petit Basset Griffon

*Correspondence to: Kayanuma, H.: kayanuma@azabu-u.ac.jp

©2020 The Japanese Society of Veterinary Science



This is an open-access article distributed under the terms of the Creative Commons Attribution Non-Commercial No Derivatives (by-nc-nd) License. (CC-BY-NC-ND 4.0: <https://creativecommons.org/licenses/by-nc-nd/4.0/>)

Vendéen (1), Bulldog (1), French Bulldog (1), Border Collie (1), Polish Lowland Sheepdog (1), Boston Terrier (1), Leonberger (1), and mixed breeds (14). The underlying diseases in these dogs were chronic nasal cavity flame (20 cases), non-neoplastic epulis (five cases), dental disease (15 cases), non-neoplastic ear canal disease (five cases), atlantoaxial subluxation (three cases), intervertebral disk disease (nine cases), diffuse liver disease (13 cases), nodular hyperplasia of liver (four cases), occlusive biliary tract obstruction (ten cases), portsystemic shunt (six cases), pancreatitis (two cases), intramuscular lipoma (two cases), and fracture of femur (one case), and no abnormality was identified during the medical examination of five dogs.

CT images (Bright Speed Elite, GE Healthcare Japan; or Asteion Super4 Edition, Canon Medical Systems, previously Toshiba Medical Systems) were obtained for the analysis in helical scan with 120 kVp and 5–112 mAs. These images were reconstructed with mediastinum algorithm and the slice thickness was 1–5 mm in accordance with the Response Evaluation Criteria in Solid Tumors (RECIST) in humans and Veterinary Cooperative Oncology Group [2, 6]. All dogs were held in prone or supine position under general anesthesia with isoflurane and taken under respiratory arrest.

The target lymph nodes were cranial sternal lymph nodes (CSLN) on the cranial sternum, cranial mediastinal lymph nodes (CMLN) in the cranial mediastinum, tracheobronchial lymph nodes (TLN; left-TLN, LTLN; right-TLN, RTLN; and middle-TLN, MTLN) adjacent to the main bronchi, aortic thoracic lymph nodes (ATLN) on the vertebral end, and pulmonary lymph nodes (PLN) on the dorsal surfaces of the principal bronchi. These lymph nodes are defined as the thoracic lymph nodes in the Miller and Evans' Anatomy of the Dog textbook [3]. The position, number, size, shape, and X-ray absorption uniformity of each lymph node were evaluated using conventional CT images that better distinguish between the lymph nodes and end of vessels as well as changes in size and uniformity of lymph nodes compared to contrast CT imaging. The CT image was set to the window level (10–80) and width (400–800) suitable for soft tissues.

Lymph nodes were measured in cross section according to RECIST [2, 6]. The measurements included maximum/major diameter (L) and minor diameter (S) perpendicular to the major diameter on a cross-section (XY plane). If the same lymph node was depicted on two continuous sections, L and S were measured on the section where the size of that lymph node was at its maximum (Fig. 1). Since MTLN formed a V-shape branching into right and left legs, a lateral direction was chosen where the distance between the right and left legs was at its maximum as L and measured ventro-dorsal direction perpendicular to L as S (Fig. 2). In the present study, craniocaudal (Z-axis) size of lymph nodes was excluded from the measurement, because target lymph nodes were small, slice thickness varied and was not isotropic, and RECIST did not use craniocaudal CT images. We defined the shape as “elliptical” when $S/L < 0.5$ and “circular” when $S/L \geq 0.5$ [4, 8, 11]. X-ray absorption uniformity of lymph node was classified into uniform, non-uniform, and low X-ray absorption at the hilum of the lymph node (central low absorption) (Fig. 3). Since the size of lymph nodes depended on the size of the dog, in addition to S/L, we measured the diameter of the aorta (Ao) at the eighth rib and calculated L/Ao and S/Ao . In addition, we examined whether the size of lymph nodes correlated with the body weight or the diameter of the aorta. For dogs where multiple lymph nodes with the same name were found, the ratio was calculated using the average values of the lengths of L and S. For statistical analysis, we examined whether L and S of each lymph node correlated with the body weight and diameter of the aorta using the Pearson correlation coefficient or Spearman's rank correlation. We defined those with correlation coefficient (r_s) of 0.4–0.7 as correlated and >0.7 as strongly correlated ($P < 0.05$). Measured values were presented as mean \pm standard deviation (range), with three significant digits.

CSLN were observed in 96/100 dogs. They were observed on the dorsal side of the second and third sternebra and cranial side of the internal thoracic artery and vein, where they were present only on the right side in 2/96 dogs, on the left side in 3/96 dogs, and in the center in 4/96 dogs. In 85/96 dogs, CSLN was present on both sides. In 2/96 dogs, CSLN was present in all three locations (left, right, and center) (Fig. 4). As such, zero to three CSLN were observed in each dog, with the total of 188 in 96 dogs. The

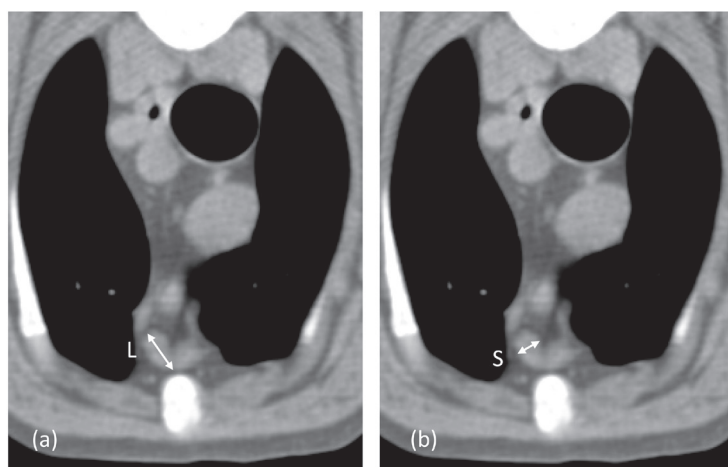


Fig. 1. (a) Long axis of sternal lymph node. (b) Short axis of sternal lymph node. Lymph node measurements included maximum diameter/major diameter (L) and minor diameter (S) perpendicular to the major diameter.

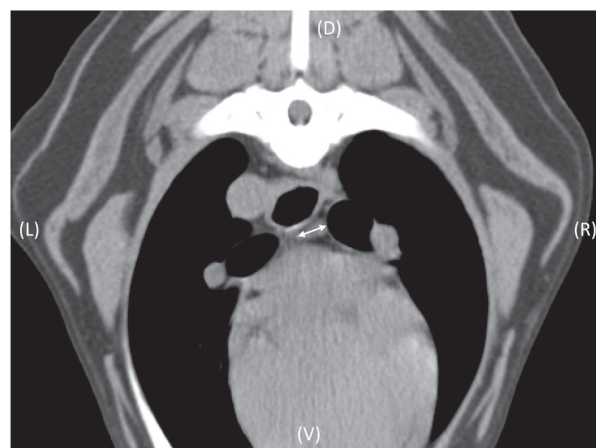


Fig. 2. Long axis of middle tracheobronchial Lymph node. (R) right, (L) left, (D):dorsal, (V) ventral.

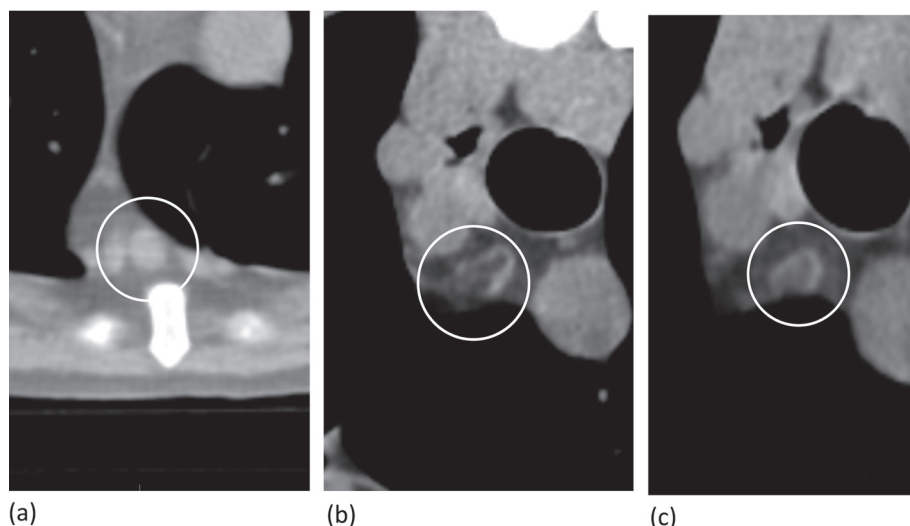


Fig. 3. Classification of X-ray absorption uniformity of Lymph node (circle) (a) uniform, (b) non-uniform, and (c) low X-ray absorption at the hilum of the lymph (central low absorption).

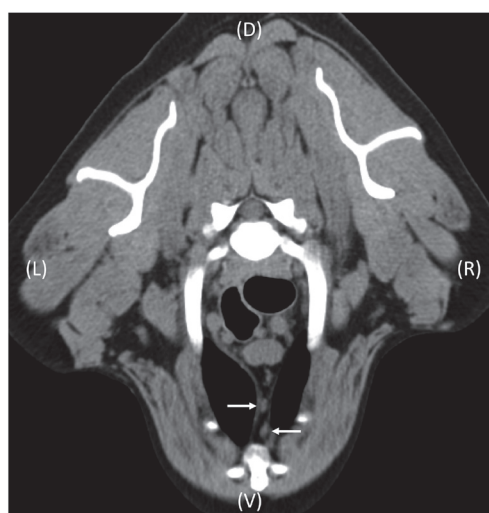


Fig. 4. Sternal lymph nodes (arrows). (R) right, (L) left, (D) dorsal, and (V) ventral.

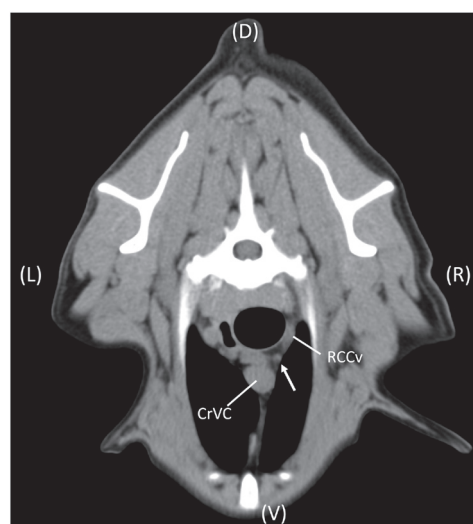


Fig. 5. Cranial mediastinal lymph node (arrow) located between cranial vena cava (CrVC) and right costocervical vein (RCCV).

mean number of CSLN observed in each dog was 1.88 ± 0.50 (range, 0–3). The mean size of the 188 lymph nodes was $L=5.15 \pm 1.89$ mm (range, 1.69–10.3 mm) and $S=3.16 \pm 1.09$ mm (range, 1.48–7.03 mm). There were 37/188 elliptical lymph nodes (20%) and 151/188 circular lymph nodes (80%). One elliptical lymph node was bimodal, and one circular lymph node had an irregular margin. Lymph node structure was uniform in 167/188 lymph nodes (89%) and non-uniform in 6/188 lymph nodes (4%). There were 13/188 lymph nodes (7%) with central low absorption.

CMLN was observed in all 100 dogs in the cranial mediastinum, especially between the right jugular veins and cranial vena cava (86/100 cases) (Fig. 5), between brachiocephalic artery and cranial vena cava (85/100 cases) (Fig. 6), and between brachiocephalic artery and left subclavian artery (57/100 cases) (Fig. 7). In some dogs, CMLN was observed along the external jugular vein, cranial vena cava, right jugular veins, common carotid artery, right subclavian artery, brachiocephalic artery, left subclavian artery, and ventral side of the trachea. In each dog, two to nine CMLN were observed, with a total of 423 lymph nodes. There were 12 dogs with two, 24 dogs with three, 27 dogs with four, 17 dogs with five, 10 dogs with six, seven dogs with seven, two dogs with eight, and one dog with nine CMLNs. The mean number of CMLN was 4.23 ± 1.57 (range, 2.0–9.0). The mean size of 423 lymph nodes was $L=4.51 \pm 1.66$ mm (range, 1.92–13.3 mm) and $S=2.74 \pm 0.79$ mm (range, 1.37–7.03 mm). Regarding shape, there were 86/423 elliptical lymph nodes (20%) and 337/423 circular lymph nodes (80%). There was one elliptical and one circular lymph node,

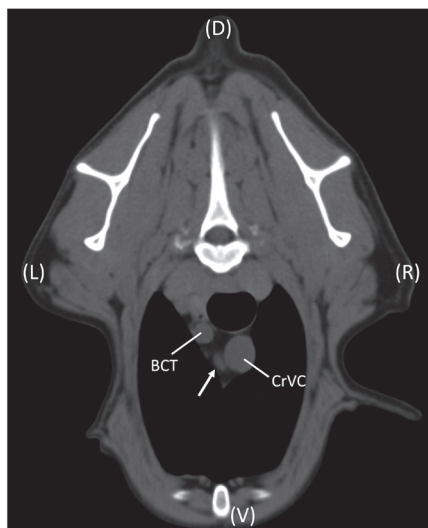


Fig. 6. Cranial mediastinal lymph node (arrow) located between brachiocephalic trunk (BCT) and cranial vena cava (CrVC). (R) right, (L) left, (D) dorsal, and (V) ventral.

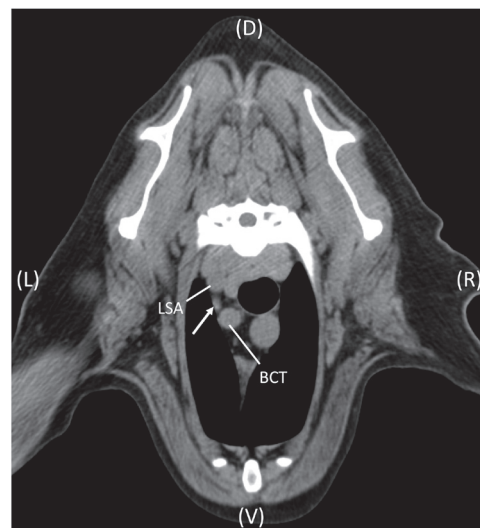


Fig. 7. Cranial mediastinal lymph node located (arrow) between brachiocephalic (BCT) trunk and left subclavian artery (LSA). (R) right, (L) left, (D) dorsal, and (V) ventral.

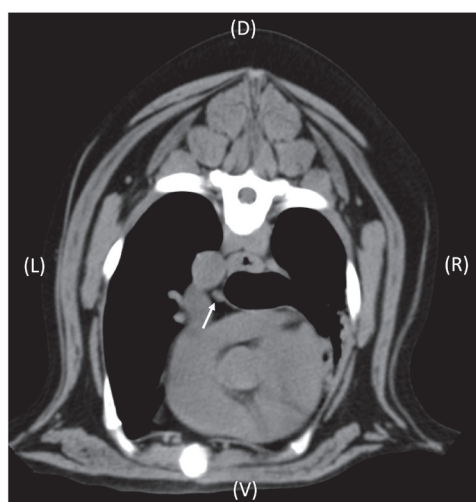


Fig. 8. Left tracheobronchial lymph node (arrow). (R) right, (L) left, (D) dorsal, and (V) ventral.



Fig. 9. Middle tracheobronchial lymph node (arrow). (R) right, (L) left, (D) dorsal, and (V) ventral.

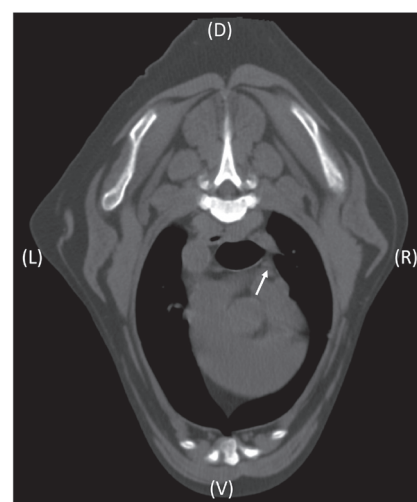


Fig. 10. Right tracheobronchial lymph node (arrow). (R) right, (L) left, (D) dorsal, and (V) ventral.

each with an irregular margin. There were 396/423 lymph nodes with uniform structure (94%) and 14/423 lymph nodes (3%) with non-uniform structure. There were 13/423 lymph nodes (3%) with central low absorption.

TLN was observed in 99/100 dogs. LTLN was observed on the dorsal side of left trachea, MTLN was observed on the dorsal side of the bifurcation of trachea, and RTLN was observed on the cranial side of the right trachea (Figs. 8–10). Zero to three TLN was observed in each dog, with a total of 275 lymph nodes. Only one TLN was observed in 5/99 dogs, two in 12/99 dogs, and three in 82/99 dogs. There were 7/100 dogs where LTLN was not observed. There was one LTLN in 93/100 dogs. MTLN was not seen in 1/100 dogs, while one MTLN was seen in 99/100 dogs. RTLN was not observed in 17/100 dogs and one RTLN was observed in 83/100 dogs. The mean number of TLN per dog was 2.75 ± 0.59 (range, 0–3). The mean size of LTLN in 93 dogs was $L=5.76 \pm 1.71$ mm (range, 2.91–10.7) and $S=3.17 \pm 0.95$ mm (range, 1.31–6.85). L of MTLN in 99 dogs was 8.79 ± 4.21 mm (range, 3.14–24.3), while S was 3.06 ± 1.05 mm (range, 1.17–6.87). L of RTLN in 83 dogs was 5.73 ± 1.79 mm (range, 2.53–12.4), while S was 3.00 ± 1.02 mm (range, 1.17–6.04). The shape of LTLN was elliptical in 38/93 lymph nodes (41%) and circular in 55/93 lymph nodes (59%), while the shape of MTLN was elliptical in 78/99 lymph nodes (79%) and circular in 21/99 lymph nodes (21%). The shape of RTLN

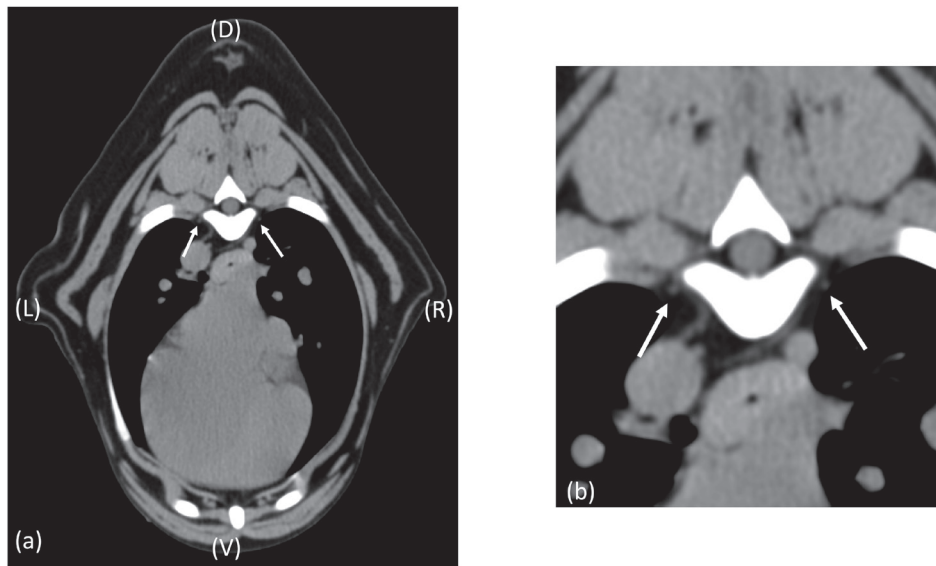


Fig. 11. Intercostal lymph nodes (arrows). (a) Conventional image. (b) Enlarged image. (R) right, (L) left, (D) dorsal, and (V) ventral.

was elliptical in 33/83 lymph nodes (40%) and circular in 50/83 lymph nodes (60%). All observed TLN were uniform.

ATLN was observed in 12/100 dogs at the vertebral end of fourth to seventh intercostal spaces (Fig. 11). In 5/12 dogs, ATLN was found on the left side, while it was found on the right side in 4/12 dogs. In 3/12 dogs, ATLN was found on both sides. Zero to 2 ATLN was observed, with a total of 16 lymph nodes. In 88/100 dogs, there were no ATLN. In 8/100 dogs, one ATLN was observed, while two lymph nodes were observed in 4/100 dogs. The mean number of ATLN per dog was 0.16 ± 0.47 (range, 0–2). The mean size of 16 ATLN was $L=2.84 \pm 1.08$ mm (range, 1.24–5.1 mm) and $S=2.19 \pm 0.79$ mm (range, 0.87–3.89 mm). Regarding shape, 1/16 ATLN was elliptical (6%) and 15/16 ATLN were circular (94%). In 15/16 lymph nodes (94%), the structure was uniform, while it was non-uniform in 1/16 lymph nodes (6%). PLN was not observed in any of the 100 dogs examined in this study.

The number of dogs and lymph nodes, measurement results, shapes, and X-ray absorption uniformity of each lymph node discussed above were summarized in Tables 1–5.

S/L obtained from actual measurements of minor diameter (S) and major diameter (L) of long lymph nodes was 0.63 ± 0.13 for CSLN, 0.63 ± 0.10 for CMLN, 0.58 ± 0.18 for LTLN, 0.40 ± 0.18 for MTLN, 0.54 ± 0.16 for RTLN, and 0.78 ± 0.1 for ATLN. L/Ao was 0.55 ± 0.15 for CSLN, 0.49 ± 0.14 for CMLN, 0.63 ± 0.16 for LTLN, 0.93 ± 0.33 for MTLN, 0.60 ± 0.14 for RTLN, and 0.29 ± 0.08 for ATLN. S/Ao was 0.36 ± 0.1 for CSLN, 0.32 ± 0.09 for CMLN, 0.37 ± 0.11 for LTLN, 0.35 ± 0.10 for MTLN, 0.33 ± 0.09 for RTLN, and 0.24 ± 0.07 for ATLN (Table 6).

We examined the correlation between the L of each thoracic lymph node and body weight, and we found that CSLN ($rs=0.64$, $P<0.05$) and MTLN ($rs=0.65$, $P<0.05$) exhibited a positive correlation, while CMLN ($rs=0.71$, $P<0.05$), LTLN ($rs=0.72$, $P<0.05$), RTLN ($rs=0.76$, $P<0.05$), and ATLN ($rs=0.75$, $P<0.05$) exhibited a strong positive correlation. When the correlation between the S of each thoracic lymph node and body weight was examined, CSLN ($rs=0.58$, $P<0.05$), LTLN ($rs=0.63$, $P<0.05$), MTLN ($rs=0.57$, $P<0.05$), RTLN ($rs=0.62$, $P<0.05$), ATLN ($rs=0.48$, $P<0.05$), and CMLN ($rs=0.68$, $P<0.05$) exhibited a positive correlation, while there was no strong positive correlation. Alternatively, the L of each thoracic lymph node and aortic diameter exhibited a positive correlation in CSLN ($rs=0.67$, $P<0.05$), CMLN ($rs=0.64$, $P<0.05$), LTLN ($rs=0.68$, $P<0.05$), MTLN ($rs=0.59$, $P<0.05$), and ATLN ($rs=0.62$, $P<0.05$), and a strong positive correlation in RTLN ($rs=0.71$, $P<0.05$). The S of each thoracic lymph node and aortic diameter exhibited a positive correlation in CSLN ($rs=0.56$, $P<0.05$), CMLN ($rs=0.59$, $P<0.05$), LTLN ($rs=0.55$, $P<0.05$), MTLN ($rs=0.53$, $P<0.05$), RTLN ($rs=0.60$, $P<0.05$), and ATLN ($rs=0.50$, $P<0.05$), but there was no strong positive correlation (Table 7).

In the present study, we observed the thoracic CT images of 100 dogs. The position of each confirmed lymph node and lymph nodes reported in macroscopic anatomy were consistent. CSLN were observed in 96/100 and 4/100 dogs were not observed on CT images. CSLN is located on the cranioventral side of internal thoracic blood vessels inside of the second costal cartilage joint, and usually there are lateral pairs of lymph nodes [3]. However, there were some dogs with only one CSLN either on the left or right side, some without any CSLN, and in rare cases, two CSLN on one side [3]. The shape was usually elliptical with the size ranging from 2 to 20 mm [3]. CMLN were observed in all dogs in this study. The number and shape of CMLN varied for each dog, but in most dogs, three to 12 CSLN were found along the cranial vena cava, brachiocephalic artery, left subclavian artery, and costocervical trunk [3]. The shapes included spindle, elliptical, and circular forms. The size was as large as 10 mm for large dogs, but usually ranged from 1 to 3 mm. It has been reported that CMLN includes those positioned along the dorsal and lateral sides of the trachea and those present on the surface of the heart [3]. However, in the present study, we did not observe the lymph nodes along the dorsal or lateral sides of the trachea and on the surface of the heart. This was possibly due to extremely small lymph nodes, making them difficult to differentiate from the longus colli muscle on the dorsal side of the trachea, from the esophagus on the lateral side, and

Table 1. Number of lymph nodes identified in thoracic computed tomography studies

Lymph node	Total number of lymph nodes (N=100 dogs)	Mean ± SD	Range	Median
Sternal	188	1.88 ± 0.50	0–3	2
Cranial mediastinal	423	4.23 ± 1.56	2–9	4
Left tracheobronchial	93	0.93 ± 0.26	0–1	1
Middle tracheobronchial	99	0.93 ± 0.10	0–1	1
Right tracheobronchial	83	0.83 ± 0.38	0–1	1
Intercostal	16	0.16 ± 0.47	0–2	0

SD, standard deviation.

Table 2. Number of dogs with 0–9 lymph nodes

	Number of lymph nodes									
	0	1	2	3	4	5	6	7	8	9
Sternal	4	7	86	3						
Cranial mediastinal	0	0	12	24	27	17	10	7	2	1
Tracheobronchial	1	5	12	82						
Intercostal	88	8	4							

Table 3. Range of lymph node long distance and short distance

	Long lengths (mm)	Short lengths (mm)
Sternal	5.15 ± 1.89 (1.69–10.3, 4.67)	3.16 ± 1.09 (1.48–7.03, 2.87)
Cranial mediastinal	4.51 ± 1.66 (1.92–13.3, 4.15)	3.16 ± 1.09 (1.48–7.03, 2.87)
Left tracheobronchial	5.76 ± 1.71 (2.91–10.7, 5.35)	3.17 ± 0.95 (1.31–6.85, 3.10)
Middle tracheobronchial	8.79 ± 4.21 (3.14–24.3, 7.54)	3.06 ± 1.05 (1.17–6.87, 2.99)
Right tracheobronchial	5.73 ± 1.79 (2.53–12.4, 5.26)	3.00 ± 1.02 (1.17–6.04, 2.82)
Intercostal	5.15 ± 1.89 (1.69–10.3, 4.67)	2.19 ± 0.79 (0.87–3.89, 2.26)

Mean ± standard deviation (range, median).

Table 4. Number of lymph nodes detected for each shape classification group

Lymph node	Elliptical (%)	Circular (%)
Sternal	37 ^{a)} (20%)	151 ^{b)} (80%)
Cranial mediastinal	86 ^{b)} (20%)	337 ^{b)} (80%)
Left tracheobronchial	38 (41%)	55 (59%)
Middle tracheobronchial	78 (79%)	21 (21%)
Right tracheobronchial	33 (40%)	50 (60%)
Intercostal	1 (6%)	15 (94%)

a) Includes one bilobar lymph node; b) Includes one lymph node with an irregular margin.

Table 5. Number of lymph nodes detected for each structure classification group

Lymph node	Uniform (%)	Non-uniform (%)	Central low absorption (%)
Sternal	167 (89%)	8 (4%)	13 (7%)
Cranial mediastinal	396 (94%)	14 (3%)	13 (3%)
Tracheobronchial	275 (100%)	0 (0%)	0 (0%)
Intercostal	15 (94%)	1 (6%)	0 (0%)

Table 6. Value of each ratio

Lymph node	Short distance/long distance of lymph node	Long distance of lymph node/aorta diameter	Short distance of lymph node/aorta diameter
Sternal	0.63 (± 0.13)	0.55 (± 0.15)	0.36 (± 0.11)
Cranial mediastinal	0.63 (± 0.10)	0.49 (± 0.14)	0.32 (± 0.09)
Left tracheobronchial	0.58 (± 0.18)	0.63 (± 0.16)	0.37 (± 0.11)
Middle tracheobronchial	0.40 (± 0.18)	0.94 (± 0.33)	0.35 (± 0.10)
Right tracheobronchial	0.54 (± 0.16)	0.60 (± 0.14)	0.33 (± 0.09)
Intercostal	0.78 (± 0.12)	0.29 (± 0.08)	0.24 (± 0.07)

(± standard deviation).

Table 7. Correlation of lymph node and body weight and aortic diameter

Lymph node	Lengths	Body weight ($P < 0.05$)	Aortic diameter ($P < 0.05$)
Sternal	L	0.64	0.67
	S	0.58	0.56
Cranial mediastinal	L	0.71	0.64
	S	0.68	0.59
Left tracheobronchial	L	0.72	0.68
	S	0.63	0.55
Middle tracheobronchial	L	0.65	0.59
	S	0.57	0.54
Right tracheobronchial	L	0.76	0.71
	S	0.62	0.6
Intercostal	L	0.75	0.62
	S	0.48	0.5

L, Long; S, short.

from the boundary of the heart. TLN consisted of MTLN, LTLN, and RTLN, where RTLN and LTLN were located outside the bronchial tube, branching into left and right from the trachea. RTLN was located on the ventral side of the azygos vein, while LTLN was located on the caudal side of the origin of the aortic arch. The shape was elliptical, with a size of 5 to 30 mm in the craniocaudal direction [3]. MTLN was found on the caudal side of the left and right main bronchi, with a V-shape and the largest size among

TLNs [3]. In this study, TLN was confirmed in 99/100 dogs, specially MTLN and LTLN were confirmed at a high rate (99/100 and 93/100 dogs, respectively). RTLN had a lower detection rate at 83/100 dogs. RTLN was probably sandwiched by structures such as azygos vein and caudal vena cava, and as the lymph nodes overlapped with these structures, the detection became difficult. ATLN is anatomically found near the ventral side of the outer vertebrate between the fifth and sixth intercostal space [3]. In 25% of dogs, ATLN was visually confirmed, and 4% of dogs had ATLN on both sides [3]. However, in the present study, ATLN was only found in 12% of dogs. Because ATLN has different number of nodes in each dog, it is possible that ATLN were not present in many of the dogs in this study, or they were extremely small and difficult to differentiate as they overlapped with longus colli, intercostal arteries, and veins near ATLN. PLNs are small lymph nodes present on the dorsal surface of left and right main bronchi between left RTLN and left and right lung parenchyma [3]. Many dogs are missing PLN, with one study reporting that only 14 of 41 dogs had them, and no dog had PLN on both sides [3]. PLNs were not observed in the present study. Since many dogs do not have PLNs or they are extremely small and close to lung parenchyma, they may not have been observed in this study due to a partial-volume effect.

In this study, there was a positive correlation between L and S of lymph nodes with body weight or aortic diameter. However, the size of lymph nodes varied widely between dogs. The mean \pm standard deviation of all calculated S/L, L/Ao, and S/Ao presented large variations, it was difficult to set the clinical reference values for lymph nodes that accounted for the size of the dog on CT scans as in existing reports.

In previous reports, a circular shape was an abnormal finding [4, 7, 9, 12, 13]. In the present study, we only examined cross sections and did not evaluate the shape in the craniocaudal direction. However, when we evaluated the shape with S/L, there were more circular lymph nodes than elliptical lymph nodes in all types of lymph nodes, except MTLN. As such, circular lymph nodes may not indicate abnormality in dogs. In addition, heterogeneous lymph nodes and lymph nodes with central low absorption or central low echo were both considered abnormal findings in earlier studies [1, 9, 13]. In the present study, in all lymph nodes other than TLN, there were 3%–6% non-uniform lymph nodes and 3–7% lymph nodes with central low absorption. Therefore, care must be taken to distinguish between non-uniform lymph nodes without a pathological sign and heterogeneous lymph nodes with pathological signs. There was fat and a lymphatic sinus at the hilum of lymph nodes, which could have led to lower CT values at the center than the margin. However, since CT scan could differentiate solids versus liquids and soft tissues versus fats, heterogeneity of the lymph nodes was more apparent in CT compared to that using X-ray examinations or ultrasound.

In the present study, we analyzed thoracic CT images of 100 dogs without any lesions in the areas of each thoracic lymph node. We examined the position, number, size, shape, and uniformity of intrathoracic lymph nodes. The results showed that the position, number, and size of lymph nodes varied among dogs. Consistent with macroscopic anatomical studies, these lymph nodes could be observed in CT scans. In addition, like previous reports, it was difficult to set a clinical index associated with lymph node size that accounted for the dog size using CT scans. Imaging findings that indicated abnormalities, such as circular shapes and non-uniformity or heterogeneity, may be routinely found in dogs in CT scans. In studies such as the present one, it is impossible to verify the pathological health in all observed lymph nodes. To determine a more accurate diagnostic index, a larger number of CT findings and pathological findings need to be analyzed and compared to dogs with abnormalities in thoracic lymph nodes.

REFERENCES

1. Ballegeer, E. A., Adams, W. M., Dubielzig, R. R., Paoloni, M. C., Klauer, J. M. and Keuler, N. S. 2010. Computed tomography characteristics of canine tracheobronchial lymph node metastasis. *Vet. Radiol. Ultrasound* **51**: 397–403. [Medline] [CrossRef]
2. Beukers, M., Grosso, F. V. and Voorhout, G. 2013. Computed tomographic characteristics of presumed normal canine abdominal lymph nodes. *Vet. Radiol. Ultrasound* **54**: 610–617. [Medline]
3. Bezuidenhout, A. J. 2013. The lymphatic system. pp. 545–550. In: *Anatomy of the Dog* 4th ed. (Evans, H. E. and Lahunta, L. eds.), Elsevier, St. Louis.
4. De Swarte, M., Alexander, K., Rannou, B., D'Anjou, M. A., Blond, L. and Beauchamp, G. 2011. Comparison of sonographic features of benign and neoplastic deep lymph nodes in dogs. *Vet. Radiol. Ultrasound* **52**: 451–456. [Medline] [CrossRef]
5. Dobson, J. M. 2003. TMN classification and clinical staging. p.18. In: *BSAVA Manual of Canine and Feline Oncology* 2nd ed. (Dobson, J. M. and Lascelles, B. D. X. eds), British Small Animal Veterinary Association, Gloucester.
6. Eisenhauer, E. A., Therasse, P., Bogaerts, J., Schwartz, L. H., Sargent, D., Ford, R., Dancey, J., Arbuck, S., Gwyther, S., Mooney, M., Rubinstein, L., Shankar, L., Dodd, L., Kaplan, R., Lacombe, D. and Verweij, J. 2009. New response evaluation criteria in solid tumours: revised RECIST guideline (version 1.1). *Eur. J. Cancer* **45**: 228–247. [Medline] [CrossRef]
7. Llabrés-Díaz, F. J. 2004. Ultrasonography of the medial iliac lymph nodes in the dog. *Vet. Radiol. Ultrasound* **45**: 156–165. [Medline] [CrossRef]
8. Nguyen, S. M., Thamm, D. H., Vail, D. M. and London, C. A. 2015. Response evaluation criteria for solid tumours in dogs (v1.0): a Veterinary Cooperative Oncology Group (VCOG) consensus document. *Vet. Comp. Oncol.* **13**: 176–183. [Medline] [CrossRef]
9. Nyman, H. T., Kristensen, A. T., Skovgaard, I. M. and McEvoy, F. J. 2005. Characterization of normal and abnormal canine superficial lymph nodes using gray-scale B-mode, color flow mapping, power, and spectral Doppler ultrasonography: a multivariate study. *Vet. Radiol. Ultrasound* **46**: 404–410. [Medline] [CrossRef]
10. Paoloni, M. C., Adams, W. M., Dubielzig, R. R., Kurzman, I., Vail, D. M. and Hardie, R. J. 2006. Comparison of results of computed tomography and radiography with histopathologic findings in tracheobronchial lymph nodes in dogs with primary lung tumors: 14 cases (1999–2002). *J. Am. Vet. Med. Assoc.* **228**: 1718–1722. [Medline] [CrossRef]
11. Smeets, A. J., Zonderland, H. M., van der Voorde, F. and Laméris, J. S. 1990. Evaluation of abdominal lymph nodes by ultrasound. *J. Ultrasound Med.* **9**: 325–331. [Medline] [CrossRef]
12. Tohnosu, N., Onoda, S. and Isono, K. 1989. Ultrasonographic evaluation of cervical lymph node metastases in esophageal cancer with special reference to the relationship between the short to long axis ratio (S/L) and the cancer content. *J. Clin. Ultrasound* **17**: 101–106. [Medline] [CrossRef]
13. Toriyabe, Y., Nishimura, T., Kita, S., Saito, Y. and Miyokawa, N. 1997. Differentiation between benign and metastatic cervical lymph nodes with ultrasound. *Clin. Radiol.* **52**: 927–932. [Medline] [CrossRef]